NEUROSCIENCE

Therapy using implanted organic bioelectronics

10.1126/sciadv.1500039

Amanda Jonsson,[1]* Zhiyang Song,[2]* David Nilsson,[3] Björn A. Meyerson,[2] Daniel T. Simon,[1]† Bengt Linderoth,[2] Magnus Berggren[1]

Many drugs provide their therapeutic action only at specific sites in the body, but are administered in ways that cause the drug's spread throughout the organism. This can lead to serious side effects. Local delivery from an implanted device may avoid these issues, especially if the delivery rate can be tuned according to the need of the patient. We turned to electronically and ionically conducting polymers to design a device that could be implanted and used for local electrically controlled delivery of therapeutics. The conducting polymers in our device allow electronic pulses to be transduced into biological signals, in the form of ionic and molecular fluxes, which provide a way of interfacing biology with electronics. Devices based on conducting polymers and polyelectrolytes have been demonstrated in controlled substance delivery to neural tissue, biosensing, and neural recording and stimulation. While providing proof of principle of bioelectronic integration, such demonstrations have been performed in vitro or in anesthetized animals. Here, we demonstrate the efficacy of an implantable organic electronic delivery device for the treatment of neuropathic pain in an animal model. Devices were implanted onto the spinal cord of rats, and 2 days after implantation, local delivery of the inhibitory neurotransmitter γ-aminobutyric acid (GABA) was initiated. Highly localized delivery resulted in a significant decrease in pain response with low dosage and no observable side effects. This demonstration of organic bioelectronics-based therapy in awake animals illustrates a viable alternative to existing pain treatments, paving the way for future implantable bioelectronic therapeutics.

INTRODUCTION

Chronic pain is a major health problem that affects 30% of the population, and about 7% suffer from neuropathic pain (*1*). This type of pain arises from lesions, dysfunctions, or other perturbations of the peripheral or central nervous system (PNS or CNS), and is characterized by spontaneous pain or amplified pain responses. The disease often leads to considerable individual suffering, as well as a financial burden to society (*2*, *3*). Despite extensive research, neuropathic pain remains one of the most difficult challenges for physicians, and almost half of the patients in routine clinical practice experience unsatisfactory pain relief (*4*). There are a variety of factors leading to the low effectiveness of chronic pain pharmacotherapy, one being the systemic administration of the drugs. With systemic administration, only a fraction of the drug reaches the targeted mechanisms, whereas the remainder of the dosage may cause adverse effects elsewhere in the body.

When pain is experienced, signals travel along sensory neurons from the site of injury, via the spinal cord, to the brain. The spinal cord is a crucial waypoint in the pain signaling pathway, because it is here, at the dorsal horn, that the sensory neurons transmit the signal from the PNS to the CNS, and ultimately into the brain. A promising means for interfering with pain signaling—and thus effecting therapy—would be to deliver therapeutics precisely at the spinal cord where these signals are transmitted between neurons. Indeed, opioids and other substances have been delivered in just this way, directly to the cerebrospinal fluid surrounding the spinal cord. Compared to systemic therapies, this method reduces the required dosage and thus the side effects. However, with this route of administration, it is not possible to target a limited section of the spinal cord (*5*), but instead, the therapeutic spreads to large parts of the CNS, sometimes leading to serious side effects.

In neuropathic pain, the pain signaling has become perturbed. In particular, there is evidence that a dysfunctional GABAergic (γ-aminobutyric acid) system is related to the occurrence of spontaneous pain and amplified pain responses observed in neuropathic pain (*6*, *7*). GABA is the primary inhibitory neurotransmitter in the CNS, and we have previously demonstrated, using microdialysis, that after nerve injury, the amount of extracellular GABA is reduced in the dorsal horns corresponding to the injured nerve (*8*, *9*). The reduced level of GABA suggests that the inhibition of pain signals is not functioning, which may partly explain the exaggerated pain experienced after nerve injury. To restore inhibitory pain control, liquid medium carrying GABA or baclofen, a $GABA_B$ receptor agonist, can be infused to the cerebrospinal fluid (*10*, *11*). As discussed previously, however, the drugs will spread to large parts of the CNS with this method, and it is not possible to target the specific part of the spinal cord corresponding to the nerve injury.

Here, however, we aimed to achieve exactly this form of precise targeting at the locations where the injured nerve root fibers enter the spinal cord. We developed an implantable device that translates electric current into the precise delivery of GABA. The device exhibits the required spatial resolution and lack of liquid flow, and was specifically designed for the anatomy of an animal model of neuropathic pain, the spared nerve injury (SNI) model (*12*). In the SNI model, pain signals originate from lesions at branches of the sciatic nerve and from sensitized and hyperreactive secondary cells in the respective dorsal horns. The pain signals travel along the sciatic nerve and enter the dorsal spinal cord at four locations at the lumbar level. The delivery device was thus designed for simultaneous, highly localized delivery of GABA to these four points. The device is a variant of the organic electronic ion pump (OEIP) (*13*–*15*), previously used to stimulate cells in vitro with various signaling substances including metal ions (*15*) and neurotransmitters (*13*), as well as in vivo for acute modulation of sensory function via the neurotransmitter glutamate (*14*). Compared to diffusion-based drug delivery systems, OEIPs release the therapeutic at a controlled rate only when electronically addressed.

[1]Laboratory of Organic Electronics, Department of Science and Technology, Linköping University, SE-601 74 Norrköping, Sweden. [2]Department of Clinical Neuroscience, Karolinska Institutet, SE-171 77 Stockholm, Sweden. [3]Acreo Swedish ICT AB, SE-601 17 Norrköping, Sweden.
*These authors contributed equally to this work.
†Corresponding author. E-mail: daniel.simon@liu.se

We report here on the development and characterization of the implantable device. We further demonstrate its efficacy in reducing pathological hypersensitivity by the highly localized delivery of the neurotransmitter GABA in awake, freely moving animals.

RESULTS

The design of an OEIP specifically for the SNI model in rats must take into account the rodent's specific anatomy. In the rat, the afferent sciatic nerve fibers enter the spinal cord via the four dorsal roots at spinal levels L3-L6. It is in these segments that the levels of GABA have been observed to be reduced after nerve injury (*8*). We therefore designed the OEIP in such a way that, once implanted, delivery would be concentrated to these four dorsal root segments (Fig. 1).

The OEIP is based on a thin layer of the conducting polymer poly(3,4-ethylenedioxythiophene) blended with the polyelectrolyte poly(styrenesulfonate) (PEDOT:PSS) on a polyethylene terephthalate (PET) substrate, encapsulated by an ionic and electronic insulator. PET has a long history in biomedical application (*16*, *17*) and was thus considered a viable substrate material for the given application. The PEDOT:PSS was photolithographically patterned into the desired delivery channel configuration (Fig. 1), and chemically overoxidized, disabling the electronic conductivity of the PEDOT component. The PSS, however, maintained cation-selective ionic conductivity. The resulting strip of patterned PEDOT:PSS on PET was then encapsulated with an ultraviolet (UV)–curable dielectric, and mounted in one end of a flexible tube forming the reservoir for the transported substance (for example, GABA). A PEDOT:PSS electrode was mounted in the other end of the tube, and the ends of the tube were sealed by heat crimping (Fig. 1A). When voltage is applied, the PEDOT:PSS electrode in the OEIP is oxidized, and the PEDOT:PSS counter electrode is reduced. The overoxidized, cation-selective channel forms a salt bridge, enabling unidirectional electrophoretic transport of cations (for example, $GABA^+$) out of the reservoir through the channel outlets.

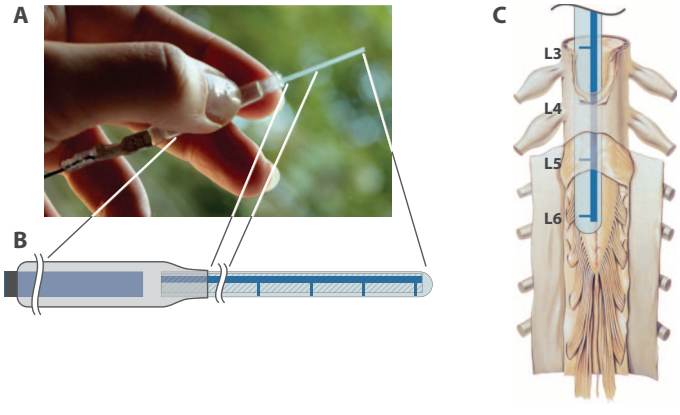

Fig. 1. The implantable OEIP and its spinal target. (**A**) Photograph of the device. (**B**) Schematic illustration: electrical connection (left); reservoir with internal electrode (center); delivery channel and outlets (right). Total length 120 mm; reservoir diameter 6 mm, length 60 mm; delivery tip width 1.2 mm, length 40 mm, thickness about 0.2 mm. (**C**) Depiction of the four outlets aligned with the sites where the sciatic nerve bundles enter the spinal cord [reused with permission from (*24*)]. The figure shows a human spinal cord, but the roots L3-L6 refer to the root levels of a rat spinal cord.

The specific geometry (Fig. 2) was achieved by modeling the equivalent circuit as a network of resistors, with the aim of achieving simultaneous delivery from four points. The ionic resistance in an electrophoretic transport channel depends on the geometry, especially the length/width ratio, and on the mobility of the particular ion. With these principles in mind, we designed the device so that the main channel leading from the reservoir to the four outlets was significantly wider than the outlet channels leading to the four delivery points (Fig. 2). The ionic resistance of each delivery "finger," R_D, based on previous measurements of GABA transport in OEIPs, was roughly two to three times higher than the resistance in the GABA supply channels, R_G. Considered as a resistor network, this results in simultaneous GABA delivery from the four points, with about two to three times higher delivery rate from the delivery point closest to the reservoir than the one farthest.

To verify that ions could be electrophoretically transported and released at the four delivery points, we first tested the transport of H^+. The reservoir was filled with aqueous HCl solution, and the device was placed in a solution containing pH indicator. The results of this transport are shown in Fig. 3. After about 2 mC of charge was transported, a color change could be observed, indicating that H^+ was successfully delivered through all four delivery points. The time delay is due to the fact that the PSS channel was initially loaded with ions other than H^+ (mostly Na^+) from the fabrication steps. The two to three times higher delivery rate estimated for the delivery point closest to the reservoir can be seen in the slightly larger ΔpH at that delivery point.

Because unidirectional cation transport through the delivery channel completes the electrical circuit in the device, the integrated current passed through the circuit (measured via the control hardware) should thus correlate with the amount of ions delivered. The OEIP GABA transport efficiency can then be defined as the ratio of $GABA^+$ transported to the number of electrons determined from the integrated supply current. Ideally, this efficiency reaches 100% when all the cur-

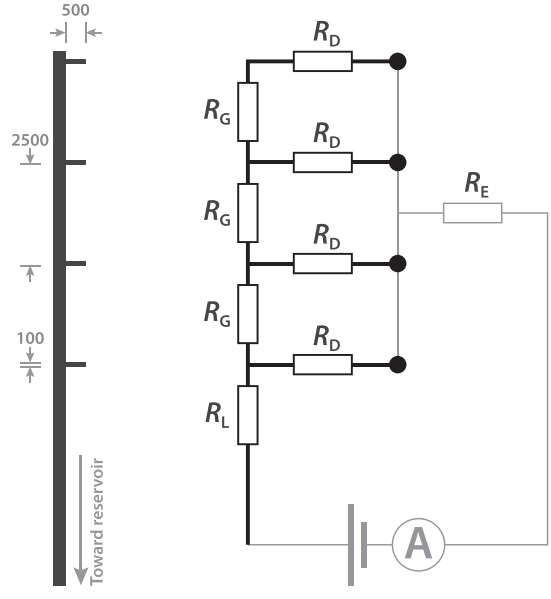

Fig. 2. Geometry of the implantable device. (**Left**) The pattern of the delivery channel leading from the reservoir out to the four delivery points (ends of the "fingers"). Dimensions are given in micrometers. (**Right**) A simplified equivalent circuit. $R_L > R_D > R_G \gg R_E$, where R_E represents the ionic resistance of the electrolyte and counter electrode.

rent passed through the cation-selective PSS channel corresponds to GABA transport. However, ion exchange membranes such as the hydrated PSS channel are never 100% permselective to cations, thus, some negative ions may migrate in the opposite direction. Also, the pH of the GABA solution was adjusted to pH 4 to achieve a high $GABA^+/H^+$ ratio (pK_a of GABA about 4.2), but given the high mobility of H^+, some H^+ are likely transported, reducing the GABA efficiency.

Using mass spectrometry, we analyzed the efficiency of planar, nonimplantable devices, made from similar materials but having different geometries than the devices used in this study. The efficiency was found to be 11 ± 1% (SD, 10 samples). For the in vivo devices used in this study, we found a similar efficiency, but a higher variation between samples: 8.6 ± 11% (SD, 28 samples). No GABA was detected when no current had been passed through devices left overnight in electrolyte (two samples), demonstrating the devices' resistance to passive leakage. Regardless of the difficulties in ascertaining an exact amount of GABA delivery, in light of the successful operation with H^+ transport above, and the in vivo results below, it is clear that significant amounts of the substance could be successfully transported.

We started the in vivo tests by creating the SNI rat model of neuropathic pain, that is, we tightly ligated and removed a few millimeters of the distal nerve stumps of the tibial and common peroneal nerves but left the sural branch intact (*12*). After nerve injury, we regularly assessed tactile sensitivity to investigate whether the rat had developed pathological hypersensitivity. Tactile hypersensitivity in rats has been demonstrated to arise shortly after creating the SNI model, and the hypersensitivity has been shown to persist for up to about 6 months (*12*). The tactile sensitivity test was performed by applying von Frey filaments with increasing stiffness to the paw corresponding to the nerve injury, and noting at what force the rat started to withdraw the paw (for details, see Materials and Methods). This hypersensitivity is considered to mimic the allodynia (pain response to innocuous stimuli such as touch) demonstrated by at least 20% of patients suffering from neuropathic pain. We implanted the OEIPs and counter electrodes in the rats that had developed tactile hypersensitivity, as evaluated 2 weeks after nerve injury. After OEIP implantation, the rats were allowed to recover for at least 48 hours before GABA delivery was started. A constant current, producing a stable GABA delivery rate, was supplied, and the withdrawal responses to tactile stimuli were assessed every 15 min. The experiment was repeated in seven separate animals. As a negative control, the same experiment was performed except that H^+ instead of $GABA^+$ was delivered in four negative control animals. The withdrawal thresholds (WTs) as a function of delivered electric charge—corresponding to $GABA^+$ or H^+ delivery—are shown in Fig. 4. It is clear that the GABA delivery elicited a significant effect, whereas the control H^+ delivery produced no change in the WTs. After about 2 to 3 mC of GABA delivery, corresponding to a maximum of 20 to 30 nmol GABA (assuming maximum efficiency), the therapeutic effect becomes evident with a clear increase of the WTs. In comparison, previous studies that used bolus injections of about 5 µmol of GABA required addition of 10 µl of solution to the cerebrospinal fluid to achieve similar WTs (*10*). Thus, even assuming the highest possible transport efficiency, OEIP delivery of GABA resulted in increased WTs with less than 1% of the amount used in intrathecal administration. Although there were differences in the effect between animals, all seven of the tested rats did respond to GABA delivery.

To verify that the implantation of the OEIP had not induced any spinal cord injury, the tactile sensibility of both the injured and noninjured side was examined. For the noninjured side, the sensitivity was always normal, that is, stable above von Frey 120-mN bending force, and not altered by the ion delivery. The side effects of GABA (and baclofen) overdose are drowsiness and muscle weakness. The rats in the present study were observed during the entire experiment for any signs of overdose. We observed no signs of interference with motor

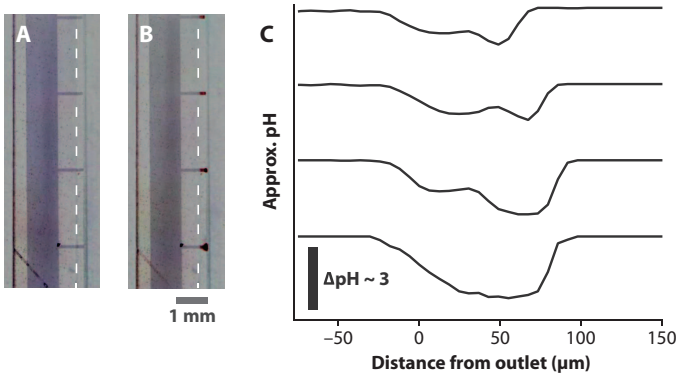

Fig. 3. Demonstration of simultaneous delivery using pH. (**A** and **B**) Microscope images of the delivery tip (A) before and (B) during delivery of H^+. The dashed lines indicate the edge of the encapsulation, defining the delivery points. The scale bar refers to both (A) and (B). The clouds of lower pH can be seen as the red regions at the delivery tips. (**C**) Approximate pH profiles at the four delivery tips. The change in pH shows the highly localized regions of lower pH.

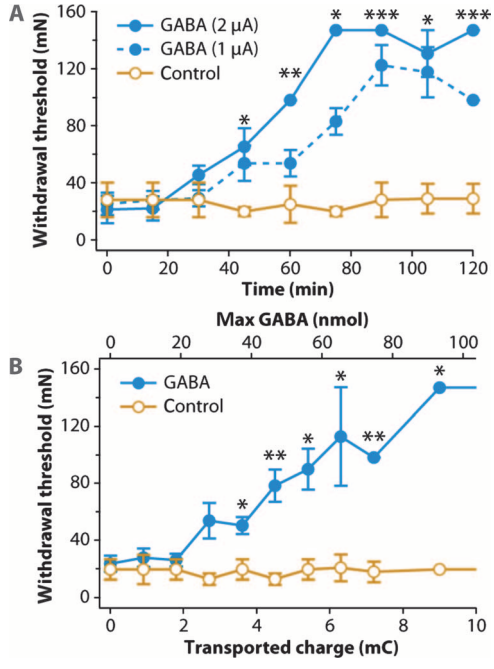

Fig. 4. Therapeutic effect of GABA delivery in vivo. (**A**) WT as a function of time for OEIP delivery of GABA at two delivery rates and H^+ control delivery. The asterisks indicate significance of multiple comparisons between all three traces. P = 0.0024, 0.0014, 0.0286, 0.0002, 0.0113, and 0.0002 for 45, 60, 75, 90, 105, and 120 min, respectively. (**B**) WT as a function of delivered therapeutic. P = 0.0303, 0.0079, 0.019, 0.0179, 0.0079, and 0.0286 for 3.6, 4.5, 5.4, 6.3, 7.2, and 9.1 mC, respectively. Data in both (A) and (B) are represented as means ± SEM.

function, for example, walking difficulties or slowing of the paw withdrawal, even at the highest GABA dosages.

DISCUSSION

To the best of our knowledge, this work illustrates the first use of an implantable organic electronic device for therapeutic purposes in a living, awake, and freely moving animal. The device was developed simultaneously as an electronic circuit (a resistor network) and as a delivery device matching a specific physiological geometry. In the specific context of treating neuropathic pain, the OEIP compares favorably with existing treatment methods. Compared to systemic administration of pharmaceuticals or administration directly to the spinal cord (intrathecally or epidurally), the OEIP targets the location of key mechanisms of the disease with a much higher spatial resolution, potentially abrogating side effects commonly observed with systemic dosages. The OEIP-based therapy also compares favorably with spinal cord stimulation (SCS), which can also be considered as an in vivo delivery algorithm because the local electrical activation of neurons results in release of various neurotransmitters such as GABA. However, at present, there is no way to specifically control the amount and relative concentration "administered" by the SCS method. This may be one reason why there are nonresponding individuals both clinically and in animal SCS experiments (*8*, *18*). In contrast, single species of therapeutic substances can easily be administered with the OEIP, providing a means of interaction with a specific biochemical pathway. With enhanced spatiotemporal resolution and biochemical specificity, the OEIP-based therapy can thus provide significant advantages over both pharmaceutical and electroceutical therapies currently available.

In these initial in vivo experiments, an excess of GABA was delivered by the OEIP to ascertain the efficacy of the technology. Future experiments can reduce the amount of GABA delivered to investigate the minimum amount required to produce a therapeutic effect. Indeed, with more precise characterization of the GABA transport efficiency, such an experiment could shed light on the specific number of GABA molecules required to achieve pain relief.

From the perspective of device design, fully implantable OEIP systems can be developed with miniaturized delivery channels and reservoirs. The lifetime of the device is limited by the capacity of the PEDOT electrodes. To increase the lifetime, an ionic current rectifier based on ion bipolar membrane diodes can be implemented in the circuit (*19*). An ionic current rectifier allows unidirectional cation transport while alternating between oxidizing and reducing the PEDOT electrodes. Therefore, with a rectifier incorporated into the circuit, the electrodes no longer limit the lifetime. Instead, the amount of substance in the reservoir would be the limiting factor. By placing the reservoir subcutaneously and by fitting it with a membrane for punctuation with an injection needle, refilling the reservoir would be possible. This type of refillable reservoir is common, for example, in commercial intrathecal pumps (for example, Medtronic SynchroMed II), and refilling is a routine procedure.

We developed a device specifically for rats. If a similar device would be used in human pain therapy, the device would of course have to be scaled up. This would necessitate longer delivery channels, but because the channels could be made wider and thicker—by depositing a thicker film of the cation-selective material—the resistance could be tailored so that a lower driving voltage would be needed. Only the initial delivery pulse would be affected by a slower onset, because the cation-selective channel must first fill with the active substance before it can be released at the outlets. Subsequent delivery pulses would result in faster onset of substance release. The larger device geometry could also provide the opportunity to incorporate speed-enhancing preloading systems (*13*) to significantly increase temporal performance. In addition, the basic resistor network enabling simultaneous delivery from four points in the present study can be enhanced by incorporating active ionic circuitry (*20*) for individual addressing of the different delivery points. For longer-term implantation, control units resembling today's pacemaker devices could be used.

This experiment was a short-term experiment in which we wanted to verify the therapeutic effect from local delivery from an OEIP. We built our OEIPs on 200-μm-thick plastic substrates proven to support device function. Recently, Minev *et al.* compared soft neural implants with the same elasticity as the dura mater, with more stiff plastic implants—like ours—and found that the stiff implants evoked motor deficits in animals after 1 to 2 weeks (*21*). Although we did not observe any signs of spinal cord injury due to the implants, it is possible that after longer times, our implants would provoke deformations of the spine, as seen in the study by Minev *et al.* This would mean that we would need to fabricate the OEIPs on thinner and more flexible substrates. Parylene C is a flexible material that can be used to encapsulate neuronal prostheses (*22*), and a material that we have used to encapsulate OEIPs for in vitro usage (*23*). It may be possible to use parylene C as both a carrier substrate and encapsulation material for implantable OEIPs.

For a substance to be delivered with an OEIP, it must be charged and not too large (to date, a few hundred grams per mole or less). These criteria actually fit several molecules that are currently used in pain therapy. For example, baclofen, which is about twice the size of GABA (213.7 versus 103.12 g/mol), can, like GABA, be charged by varying the pH and can potentially be transported with OEIP devices. This also applies to opioids such as morphine (285.34 g/mol). Indeed, we are focusing much of our effort on expanding the substance repertoire of the OEIP and expanding its capabilities with new materials allowing even larger molecules, and thus more therapeutic applications.

With the increasing understanding of neurochemical dynamics, new techniques for interfacing and augmenting specific signaling pathways will enable a range of new therapies. We see the implantable OEIP system described above as part of a long-term vision of integrating organic "iontronic" circuitry into physiological signaling at the cell level. Effecting therapy by organic electronics in awake, freely moving animals is an important step toward this goal.

MATERIALS AND METHODS

OEIP design

The device was designed to have four 100-μm-wide delivery points separated by 2.5 mm corresponding to the four sites where the injured nerve enters the spinal cord. The part of the device being inserted subarachnoidally onto the dorsal aspect of the spinal cord was 1.2 mm wide and about 6 cm long. A reservoir was made from heat shrink tube, and an electrode connected to the outside of the animal was placed inside the reservoir. The cables through the skin were placed at a distance of 12 cm from the site of delivery in the neck region to prevent the rat from reaching them.

The ion channel was designed with the aim of having simultaneous delivery at all four outlets. To achieve this, the device was modeled as a resistor network. The ionic resistance in the ion channel depends on the geometry of the channel, especially the length/width ratio, and on the mobility of the ion. There is also evidence that larger ions (that is, larger than H^+ or Na^+) tend to experience a higher resistance for more narrow channels, given the same length/width ratio. This is likely due to less swelling perpendicular to the substrate for narrower channels, and thus less water to provide higher ionic conductivity.

Organic ion pump fabrication

A prefabricated PEDOT:PSS film on PET (Orgacon EL-350, Agfa) was cleaned with Microposit Remover 1112A (Shipley), rinsed in acetone and deionized water, and then baked at 110°C for 10 min. A protective layer of poly(methyl methacrylate) (PMMA) (4 mg/ml in diethyl carbonate) was spin-coated onto the PEDOT:PSS surface (3000 rpm), and the substrates were baked for 10 min at 110°C before Microposit S1805 photoresist (Shipley) was spin-coated, baked (110°C, 10 min), exposed with a mask aligner (Suss MA/BA 6), developed in Microposit MF-319 (Shipley), baked (110°C, 10 min), and etched using O2/CF4 plasma. Remaining photoresist and PMMA were removed by acetone (60 s), and the substrates were rinsed in deionized water and dried. Next, the patterned PEDOT:PSS films were overoxidized by a sodium hypochlorite solution [1%, v/v (aq), 40 s]. Two encapsulating layers of DuPont 5018A dielectric were screen-printed and UV-cured before the individual ion pumps were cut out, and a length of heat shrink tubing (ADW400, Kacab Teknik AB) was attached by melting the end of the tube and pressing it around the devices. Carbon contacts were painted on strips of PEDOT:PSS (Orgacon EL-350, Agfa) that were used as electrodes. One electrode (anode) was placed inside the reservoir formed by the heat shrink tube. The other (cathode, counter) electrode was placed external to the device, in electrolytic contact.

OEIP characterization

Before calibration procedures as well as implantation surgery, the devices were soaked for at least 48 hours in deionized water. In the proton transport experiments, the reservoirs were filled with 100 mM HCl (aq) solution. Devices and electrodes were put in 100 mM NaCl (aq) with added pH indicator (Fluka 36828, Sigma-Aldrich). KOH was added to adjust the pH of the NaCl solution to which ions were pumped, to obtain a slightly basic pH near 8. A voltage was applied between the electrode in the device and the electrode placed in the surrounding KOH/NaCl solution using a Keithley 2602 SourceMeter controlled via LabVIEW. In the GABA experiments, the reservoirs were filled with 100 mM GABA (aq) (Sigma-Aldrich), adjusted to pH 4 by the addition of HCl. The devices were placed in Eppendorf vials containing 100 mM NaCl (aq). A voltage of 40 V was applied between the electrode inside the reservoir and the counter electrode (strip of PEDOT:PSS on PET) placed in the Eppendorf vial. A Keithley 2602 SourceMeter was again used to source the voltage, and simultaneously recorded the current. After fixed amounts of charge (ranging from 10 to 1000 μC) had been passed through the device, the device and the electrode were transferred to another Eppendorf vial. Several samples were collected in this way from six different devices, and thereafter, the GABA content was analyzed by mass spectrometry. The efficiency of the device was estimated by calculating the amount of GABA divided by the number of electrons passed through the circuit, and averaging the values obtained from the various experiments.

Animals and anesthesia

The experiments were performed on male Wistar rats (Harlan), weighing 250 to 350 g, in accordance with protocols approved by the Local Swedish Animal Welfare Agency. The surgical procedures were performed under general anesthesia delivered through an open mask system. Anesthesia was induced by 4% isoflurane (Forene, Abbott) and maintained with 1 to 2% in a 1:1 mixture of air and oxygen at a flow rate of 2 liters/min. During surgery (for creation of nerve lesion and implantation of the device, see below), the body temperature was maintained at 37 ± 0.5°C by an automatic heating pad (CMA 150, CMA Microdialysis AB). Postoperative analgesia was provided by subcutaneous injection of carprofen (5 mg/kg) (Rimadyl, Pfizer).

Spared nerve injury

An SNI rat model was created as earlier described in detail (*12*). In short, the skin of the lateral surface of the thigh was incised, and the biceps femoris muscle was divided, exposing the sciatic nerve and its three terminal branches. After ligation and removal of 2 to 4 mm of the distal nerve stumps of the tibial and common peroneal nerves, muscle and skin were closed in two layers. In sham-operated animals, the surgical procedure was identical, except that the tibial and common peroneal nerves were left intact. In this nerve injury model, about 70 to 80% of the animals develop hypersensitivity (similar to the clinical symptom "allodynia") in the operated paw to previously innocuous tactile stimuli with a latency of about 1 to 2 weeks and with a duration of about 2 months.

Assessment of pain-related behavior

The behavioral studies were carried out under standardized conditions in a separate quiet room. After the induction of nerve injury, the sensitivity in the hind paws was regularly examined (at least twice a week). The final decision whether the rats had developed a pathological degree of hypersensitivity (see below) in the lesioned hind paw was taken 2 weeks after the nerve injury.

Tactile hypersensitivity

For the tactile sensitivity tests, the rat was placed in a circular observation Plexiglas cage equipped with a metal mesh floor and allowed to acclimatize to the environment for at least 15 min before the beginning of the experiments. Tactile sensitivity was assessed using regularly calibrated von Frey filaments (MARSTOCK nervtest) with stiffness corresponding to 4.9-, 7.8-, 14.7-, 25.5-, 39.2-, 44.1-, 53.9-, 68.6-, 83.4-, 98.1-, 123-, 147-, 181-, 196-, 216-, 255-, and 294-mN bending force to quantify the sensitivity. The filaments were applied to the mid-plantar surface of the hind paw until the filament gently bent. A brisk withdrawal of the hindlimb was considered a positive response. As a control, the WTs were also determined for the same part of the contralateral, intact paw. To avoid nociceptive sensitization, the test was always started with the softest filament and continued in ascending order of stiffness. The softest filament that produced a brisk withdrawal to at least three of five applications determined the WT. Here, only rats that had developed tactile hypersensitivity, defined as a response to a filament corresponding to 68.6 mN or less, were included in the subsequent experiments. The filament corresponding to 294 mN was selected as the cutoff level (healthy rats normally have a WT greater than 294 mN) (the procedure has previously been described in detail). Only rats that developed tactile hypersensitivity, as defined above, were selected for ion pump implantation.

Implantation of the OEIP

Before implantation, the reservoirs of the ion pumps were filled with 100 mM NaCl (aq) solution, and sodium ions were transported through the devices (using a Keithley 2602 SourceMeter) to make sure any residual ions in the channel were exchanged to sodium ions. The reservoirs were then emptied of their NaCl solution, filled with GABA solution (100 mM, pH 4), and sealed. The rats were under general anesthesia (similar to the procedure described above) during the implantation of the devices. After skin incision and gentle dissection of superficial tissues, a small laminectomy at the T10 level was made. The dura and arachnoid were carefully opened in a horizontal slit fashion. The 40-mm-long, 1.2-mm-wide, and about 200-μm-thick flexible strip delivery section of the device was inserted in the caudal direction in the dorsal subarachnoid space. The four outlets of the device were adjusted to aim at the T10-T13 vertebral levels (that is, covering the targeted root levels L3-L6 of the spinal cord) ipsilateral to the nerve injured side. The soft tissues were closed in layers, and the reservoir of the device (diameter 6 mm, length 60 mm) was placed subcutaneously at the thoracic level close to the spinal processes. The electrical lead extension was tunneled subcutaneously ending in contacts fixed to the neck skin. After OEIP implantation, the rats were allowed to recover for at least 48 hours before starting further experiments. They were kept in separate cages to avoid damage to the contacts caused by other rats. To verify that the OEIP implantations did not induce spinal cord injury, the tactile sensibility of the noninjured hind paw was also examined and found to be intact in all cases. Rats with signs of neurological sequelae after the surgery were excluded from the subsequent experiments and sacrificed.

GABA delivery

For the behavioral tests, the rats were again placed in the circular observation cage. The contacts of the OEIP were connected to a SourceMeter (Keithley 2602) capable of delivering constant current of 1 or 2 μA. The animals were able to move freely in the cage during the experiments. Throughout the entire duration (120 min) of the experiment, the withdrawal responses to tactile stimuli applied to the nerve injured hind paw were assessed every 15 min. Control experiments, with the OEIP delivering H^+, were performed in other animals.

Ethical considerations

All procedures used in the present study were examined and approved by the local ethical committee.

Statistical analysis

The changes in behavior with the treatments were compared using the nonparametric Kruskal-Wallis test followed by Dunn's post hoc test for the time-correlated data (Fig. 4A). The Mann-Whitney *U* test was used for the WT versus transported charge data (Fig. 4B). Data are presented as means ± SEM. A P value <0.05 was considered as significant in all tests. Calculations were performed using GraphPad Prism 5.0 (GraphPad Inc.).

REFERENCES AND NOTES

1. C. Toth, J. Lander, S. Wiebe, The prevalence and impact of chronic pain with neuropathic pain symptoms in the general population. *Pain Med.* **10**, 918–929 (2009).
2. M. P. Jensen, M. J. Chodroff, R. H. Dworkin, The impact of neuropathic pain on health-related quality of life: Review and implications. *Neurology* **68**, 1178–1182 (2007).
3. A. B. O'Connor, Neuropathic pain: Quality-of-life impact, costs and cost effectiveness of therapy. *Pharmacoeconomics* **27**, 95–112 (2009).
4. M. Glajchen, Chronic pain: Treatment barriers and strategies for clinical practice. *J. Am. Board Fam. Pract.* **14**, 211–218 (2001).
5. B. M. Onofrio, T. L. Yaksh, Long-term pain relief produced by intrathecal morphine infusion in 53 patients. *J. Neurosurg.* **72**, 200–209 (1990).
6. K. A. Moore, T. Kohno, L. A. Karchewski, Partial peripheral nerve injury promotes a selective loss of GABAergic inhibition in the superficial dorsal horn of the spinal cord. *J. Neurosci.* **22**, 6724–6731 (2002).
7. H. U. Zeilhofer, Loss of glycinergic and GABAergic inhibition in chronic pain—Contributions of inflammation and microglia. *Int. Immunopharmacol.* **8**, 182–187 (2008).
8. C. O. Stiller, J. G. Cui, W. T. O'Connor, E. Brodin, B. A. Meyerson, B. Linderoth, Release of γ-aminobutyric acid in the dorsal horn and suppression of tactile allodynia by spinal cord stimulation in mononeuropathic rats. *Neurosurgery* **39**, 367–374 (1996).
9. J. Castro-Lopes, I. Tavares, A. Coimbra, GABA decreases in the spinal cord dorsal horn after peripheral neurectomy. *Brain Res.* **620**, 287–291 (1993).
10. J.-G. Cui, B. Linderoth, B. A. Meyerson, Effects of spinal cord stimulation on touch-evoked allodynia involve GABAergic mechanisms. An experimental study in the mononeuropathic rat. *Pain* **66**, 287–295 (1996).
11. M. Slonimski, S. E. Abram, R. E. Zuniga, Intrathecal baclofen in pain management. *Reg. Anesth. Pain Med.* **29**, 269–276 (2004).
12. I. Decosterd, C. J. Woolf, Spared nerve injury: An animal model of persistent peripheral neuropathic pain. *Pain* **87**, 149–158 (2000).
13. K. Tybrandt, K. C. Larsson, S. Kurup, D. Simon, P. Kjall, J. Isaksson, M. Sandberg, E. Jager, A. Richter-Dahlfors, M. Berggren, Translating electronic currents to precise acetylcholine-induced neuronal signaling using an organic electrophoretic delivery device. *Adv. Mater.* **21**, 4442–4446 (2009).
14. D. T. Simon, S. Kurup, K. C. Larsson, R. Hori, K. Tybrandt, M. Goiny, E. W. Jager, M. Berggren, B. Canlon, A. Richter-Dahlfors, Organic electronics for precise delivery of neurotransmitters to modulate mammalian sensory function. *Nat. Mater.* **8**, 742–746 (2009).
15. J. Isaksson, P. Kjäll, D. Nilsson, N. D. Robinson, M. Berggren, A. Richter-Dahlfors, Electronic control of Ca^{2+} signalling in neuronal cells using an organic electronic ion pump. *Nat. Mater.* **6**, 673–679 (2007).
16. B. Mallick, Nondestructive analysis of dielectric properties: Application to ion beam irradiated tissue response microfibre. *Biomed. Mater. Eng.* **24**, 1425–1432 (2014).
17. A. Metzger, *Polyethylene Terephthalate and the Pillar™ Palatal Implant: Its Historical Usage and Durability in Medical Applications* (Medtronic Inc., Jacksonville, FL, 2009).
18. G. Lind, B. A. Meyerson, J. Winter, B. Linderoth, Intrathecal baclofen as adjuvant therapy to enhance the effect of spinal cord stimulation in neuropathic pain: A pilot study. *Eur. J. Pain* **8**, 377–383 (2004).
19. E. O. Gabrielsson, P. Janson, K. Tybrandt, A four-diode full-wave ionic current rectifier based on bipolar membranes: Overcoming the limit of electrode capacity. *Adv. Mater.* **26**, 5143–5147 (2014).
20. K. Tybrandt, R. Forchheimer, M. Berggren, Logic gates based on ion transistors. *Nat. Commun.* **3**, 871 (2012).
21. I. R. Minev, P. Musienko, A. Hirsch, Q. Barraud, N. Wenger, E. M. Moraud, J. Gandar, M. Capogrosso, T. Milekovic, L. Asboth, R. F. Torres, N. Vachicouras, Q. Liu, N. Pavlova, S. Duis, A. Larmagnac, J. Vörös, S. Micera, Z. Suo, G. Courtine, S. P. Lacour, Biomaterials. Electronic dura mater for long-term multimodal neural interfaces. *Science* **347**, 159–163 (2015).
22. C. Hassler, R. P. von Metzen, P. Ruther, T. Stieglitz, Characterization of parylene C as an encapsulation material for implanted neural prostheses. *J. Biomed. Mater. Res. B Appl. Biomater.* **93**, 266–274 (2010).
23. A. Williamson, J. Rivnay, L. Kergoat, A. Jonsson, S. Inal, I. Uguz, M. Ferro, A. Ivanov, T. A. Sjöström, D. T. Simon, M. Berggren, G. G. Malliaras, C. Bernard, Controlling epileptiform activity with organic electronic ion pumps. *Adv. Mater.* 10.1002/adma.201500482 (2015).
24. M. J. Cousins, P. O. Bridenbaugh, D. B. Carr, T. T. Horlocker, *Neural Blockade in Clinical Anesthesia and Pain Medicine* (Wolters Kluwer, Philadelphia, ed. 4, 2008).

Acknowledgments: We thank A. Richter-Dahlfors for fruitful discussions. We also thank A. Sawatdee and M. Nilsson for assistance with device fabrication. **Funding:** This work was supported by a grant from the Swedish Governmental Agency for Innovation Systems (VINNOVA, dnr 2010-00507) and by the Karolinska Institutet Funds. Additional support was provided by the Knut and Alice Wallenberg Foundation, the Swedish Research Council, and the Önnesjo Foundation. **Author contributions:** A.J. and D.N. fabricated devices. Z.S. led the surgical procedures and von Frey experiments. A.J. performed the nonbiological device characterization. B.A.M., D.T.S., B.L., and M.B. contributed to the analysis and discussions of the results. A.J., Z.S., and D.T.S. wrote the manuscript. D.T.S., M.B., and B.L. supervised the project. **Competing interests:** The authors declare that they have no competing interests.

Submitted 12 January 2015
Accepted 3 April 2015
Published 8 May 2015
10.1126/sciadv.1500039

Citation: A. Jonsson, Z. Song, D. Nilsson, B. A. Meyerson, D. T. Simon, B. Linderoth, M. Berggren, Therapy using implanted organic bioelectronics. *Sci. Adv.* **1**, e1500039 (2015).